



Research article

GLS and GOT2 as prognostic biomarkers associated with dendritic cell and immunotherapy response in breast cancer

Ruifang Yang^{a,1}, Shuo Cheng^{a,1}, Jie Xiao^c, Yujie Pei^a, Zhonglin Zhu^a, Jifa Zhang^a, Jing Feng^{a,b}, Jing Li^{a,c,*}^a Anhui University of Science and Technology Affiliated Fengxian Hospital, Shanghai, 201499, China^b The Second Affiliated Hospital, The Chinese University of Hong Kong, Shenzhen, 518172, China^c School of Laboratory Medicine and Biotechnology, Southern Medical University, Guangzhou, 510515, China

ARTICLE INFO

Keywords:

Breast cancer
Dendritic cell
Immune checkpoint
GLS1
GOT2

ABSTRACT

Breast cancer is the females' most common cancer. Targeting the immune microenvironment is a new and promising treatment method for breast cancer. Nevertheless, only a small section of patients can profit by immunotherapy, and improving the ability to accurately predict the potential for immunotherapy response is still awaiting further exploration. In this study, we found that the key factors of glutamine metabolism, glutaminase 1 (GLS) and mitochondrial aspartate transaminase (GOT2), showed opposite expression patterns in breast cancer samples. Based on the expression level of GLS and GOT2, we divided the breast cancer samples into two clusters: Cluster 2 showed GLS expressed higher and GOT2 expressed lower, whereas Cluster 1 showed GOT2 expressed higher and GLS expressed lower. GSEA showed that the clusters were related to pathways of immunity. Further analysis showed that Cluster 2 was positively associated with immunity infiltration. Through WGCNA, we identified a module strongly correlated with glutamine metabolism and immunity and identified 11 dendritic cell-associated genes involved in dendritic cell development, maturation, activation and other functions. In addition, Cluster 2 also showed higher immune checkpoint gene expression, which suggest the Cluster 2 had even better response to immunotherapy. The validation dataset could also be clustered into two groups. Cluster 2 (GLS expressed higher and GOT2 expressed lower) of the validation dataset was also positively associated with dendritic cells and a better immunotherapy response. Thus, these data indicate that GLS and GOT2 are prognostic biomarkers which closely related to dendritic cells and better reacted to immunotherapy in breast cancer.

1. Introduction

Breast cancer is the females' most common cancer in the whole world. The evaluated number of incident breast cancer cases were over 2.8 million in 2022, accounting for 31% of all new cancers, and 43,250 patients died of breast cancer [1]. Considering the highly heterogeneous features of breast cancer, treatment strategies for breast cancer vary by molecular features (such as estrogen receptor (ER), progesterone receptor (PR) and human epidermal growth factor receptor 2 (HER2)) [2], gene mutations (such as BRCA1/2 [3,4]

* Corresponding author. Anhui University of Science and Technology Affiliated Fengxian Hospital, Shanghai, 201499, China.

E-mail address: lijing228nanfang@163.com (J. Li).¹ These authors have contributed equally to this work and share first authorship.<https://doi.org/10.1016/j.heliyon.2024.e24163>

Received 16 August 2023; Received in revised form 28 November 2023; Accepted 4 January 2024

Available online 7 January 2024

2405-8440/© 2024 The Authors. Published by Elsevier Ltd. This is an open access article under the CC BY-NC-ND license (<http://creativecommons.org/licenses/by-nc-nd/4.0/>).

Abbreviations

DCs	dendritic cells
BRCA	GDC TCGA Breast Cancer dataset
BRCA	The TCGA Breast Cancer dataset
GLS1	glutaminase 1
GOT2	mitochondrial aspartate transaminase
TCGA	The Cancer Genome Atlas
GSEA	gene set enrichment analysis
ssGSEA	single-sample gene set enrichment analysis
WGCNA	weighted gene coexpression network analysis
PD1	programmed death protein 1
PDL1	programmed death ligand 1
CTLA4	cytotoxic T-lymphocyte antigen 4
TNBC	triple-negative breast cancer
MHC	major histocompatibility complex
ES-DC	embryonic stem cell-derived DCs
NK	natural killer cell
LYN	Src family tyrosine kinase
RUNX3	RUNX family transcription factor 3
MSigDB	Molecular Signatures Database
MM	membership
GS	gene significance

and PIK3CA [5]) and the immune microenvironment [6]. Among these treatment methods, targeting the immune microenvironment is a new prospective treatment strategies to breast cancer [7–9].

In the tumor immune microenvironment, dendritic cells (DCs) have pivotal roles in orchestrating natural and adaptive immunity of antitumor and have become a powerful tool for tumor immunotherapy in preclinical and clinical studies [10]. DCs catch and absorb antigens, and submit them to T lymphocytes after internalizing processing [11]. Activated dendritic cells promote CD4⁺ T cells and CD8⁺ T cells initial differentiate into specific effector T cells with distinct abilities [11], stimulate natural killer cell (NK) cells, mast cell-related cells and macrophages in the innate immune system [12,13], interact with B cells to regulate humoral immunity or indirectly induce B-cell proliferation [14,15]. DC regulation is a complex process in the immune microenvironment. After sensing incentive, DCs get into a complicated developmental procedure, which called DC maturity. This process enhances DCs transiently taking up antigens [16,17], increases the expression degree of MHC class I, class II molecules and costimulatory molecules, and secretes kinds of inflammatory cytokines and chemokines [18]. Finally, DCs migrate from tissues to draining lymph nodes [19,20]. Blocking immune checkpoint pathways is another promising means for immunotherapy [21]. There are a lot of genes participated in the immune checkpoint pathway, including PD1-related genes (PD1, PDL1 and PDL2), CTLA4-related genes (CD80, CD86 and CTLA4), other immune checkpoint genes (LAG3, TIGIT and TIM3), and agonists of T-cell activation genes (4-1BB, CD27, CD40, CD70, ICOS and OX40) [22]. The expression of these genes is critical for immune checkpoint therapeutic strategies [23]. Although targeting the immune microenvironment is a new prospective therapeutic method for breast cancer, only a small section of patients can profit by immunotherapy, and improving the ability to accurately predict the potential for immunotherapy response is still awaiting further exploration.

Glutamine, as the most abundant and commonly used amino acid, is a crucial nitrogen source and respiratory fuel in cells, including immune cells. Glutamine plays major roles in releasing secretory factors and regulating cell proliferation and maintenance [24]. Glutamine metabolism is very important for multiple biological processes, including maintaining tumor survival and progression and immune cell activation [25–27]. Glutaminase (GLS), as the first enzyme in glutamine metabolism, converts glutamine to glutamate [28]. In prostate cancer cells, GLS promotes cell proliferation and suppresses cell apoptosis [29], contributing to cancer radiosensitivity [30]. Defected GLS in vascular endothelial suppresses tumor growth and metastasis and improves the response to chemotherapy [31]. Inhibiting GLS in cancer cells can diminish cell-autonomous tumorigenesis [32] and tumor immune evasion [33]. GLS is also positively correlated with immune cell infiltration in cancer [34]. GLS is positively correlated with resting memory CD4 T cells and negatively correlated with monocytes [35]. In addition, glutamate-oxaloacetate transaminase 2 (GOT2) also has an important role in glutamine metabolism. Silencing GOT2 promotes glutamine metabolism reprogramming and hepatocellular carcinoma progression [36]. Mitochondrial glutamine metabolism inhibits senescence in a GOT2-dependent manner to support pancreatic cancer growth [37]. GOT2 can also inhibit antitumor immunity by shaping the immune microenvironment through spatially limiting both CD4⁺ and CD8⁺ T cells [38]. High GOT2 expression is positively associated with immunologically quiet subtype patients and can be used for clear-cell renal cell carcinoma immunophenotyping as a marker [39]. Nevertheless, the potential molecular mechanisms of GLS and GOT2 in breast cancer have yet to be fully elucidated.

In our study, on the basis of the expression level of GLS and GOT2, we divided the breast cancer samples into two clusters (GLS expressed lower and GOT2 expressed higher) and Cluster 2 (GLS expressed higher and GOT2 expressed lower). The Cluster 2 subset

showed a stronger association with immune infiltration. Further studies suggested that the Cluster 2 subset was positively related to dendritic cells. Through WGCNA, we identified a module strongly correlated with glutamine metabolism and immunity and identified 11 dendritic cell-associated genes. Gene association analysis and protein–protein interaction analysis suggests that these genes are correlated and positively related to GLS expression and negatively related to GOT2 expression. Cluster 2 was also positively correlated to the expression level of immune checkpoint genes, indicated that Cluster 2 has better responds to immunotherapy. The validation dataset can also be divided into two clusters based on the expression level of GLS and GOT2. The Cluster 2 was positively associated with dendritic cells and a better immunotherapy response. Thus, these results indicate that GLS and GOT2 are prognostic biomarkers correlated with dendritic cells and better react to immunotherapy in breast cancer.

2. Materials and methods

2.1. Data sources and preprocessing

The clinical and transcriptome profiling data of the GDC TCGA Breast Cancer (BRCA) dataset (dataset ID: TCGA-BRCA.htseq_fpkm.tsv) were from xena website ([https://xenabrowser.net/datapages/?cohort=GDC%20TCGA%20Breast%20Cancer%20\(BRCA\)&removeHub=https%3A%2F%2Fxena.treehouse.gi.ucsc.edu%3A443](https://xenabrowser.net/datapages/?cohort=GDC%20TCGA%20Breast%20Cancer%20(BRCA)&removeHub=https%3A%2F%2Fxena.treehouse.gi.ucsc.edu%3A443)). The clinical information of cases, containing age, gender, T stage, N stage, M stage, pathological stage, and prognosis information were gotten from the dataset. HTSeq-FPKM of 1072 primary breast cancer specimens were further analyzed with $\log_2(\text{FPKM}+1)$ transformation (supplementary R code 1.1), and performed differential analysis by using HTSeq-Counts (supplementary R code 1.2). The PAM50 subtype was downloaded from the GDC TCGA Breast Cancer (BRCA) dataset through the R package TCGAbiolinks [40]. We used stacked bar chart to estimate the correlation between two clusters and PAM50 (supplementary R code 12.1).

Expression profiling by TCGA Breast Cancer (BRCA) dataset (dataset ID: TCGA.BRCA.sampleMap/HiSeqV2) was from xena (<https://xenabrowser.net/datapages/?dataset=TCGA.BRCA.sampleMap%2FHiSeqV2&host=https%3A%2F%2Ftcga.xenahubs.net&removeHub=https%3A%2F%2Fxena.treehouse.gi.ucsc.edu%3A443>). The dataset which contained 1097 breast cancer tissues was analyzed for validation of classification, immune features and hub gene expression association in breast cancer (supplementary R code 7.1–11.1).

2.2. Immune infiltration analysis

We chose 17 glutamine-associated gene sets (119 genes) and immunological signature gene sets (21,383 genes, c7.all.v2023.1.Hs.symbols.gmt) out of the Molecular Signatures Database (MSigDB). Through the intersection of glutamine-associated genes and immune signature genes we obtained 118 genes (supplementary R code 1.4).

ESTIMATE, which the proportion of stromal cells as well as immune cells was determined according to the gene expression characteristics in tumor samples, and the microenvironment to tumor of per BRCA sample was evaluated by R software package estimate according to an article that inferred the purity of tumor and the mixture of cells about stroma and immunity from the expression data (supplementary R code 1.3) [41]. By calculating four ESTIMATE indices and setting the absolute value of the four ESTIMATE indices (Stromal Score, Immune Score, ESTIMATE Score and Tumor Purity) > 0.25 , 8 genes were finally selected (supplementary R code 2.1).

CIBERSORT computes cell composition on the basis of the expression profiles [42]. We use CIBERSORT to calculate the ratio of 10 kinds of immunocytes in breast cancer samples [43]. To generate the signature matrices for CIBERSORT, we chose marker genes of 10 kinds of immune cells according to previous reports [43–45] and the CellMarker website (<http://xteam.xbio.top/CellMarker/>). Then, the marker gene list was optimized by the Garnett [46] trained classifier in the sc-RNA dataset (GSE114725) of breast cancer [45]. After obtaining the marker gene list, the signature matrices used in CIBERSORT were generated using the sc-RNA dataset (GSE114725) (supplementary R code 4.2).

We used the R package GSVA to analysis the single-sample gene set enrichment (ssGSEA) [47], and worked out the infiltration degree of 28 kinds of immunocyte types [48] (supplementary R code 4.3).

2.3. Consensus clustering on the basis of GLS and GOT2 expression

We extracted the expression of GLS and GOT2 (supplementary R code 2.2.1) and used the R package ConsensusClusterPlus to cluster [49]. We divided the breast cancer samples into two clusters (supplementary R code 2.3).

2.4. Survival analysis

The overall survival times of patients with different subtypes were obtained from the PAM50 subtype information of the GDC TCGA Breast Cancer (BRCA) dataset. Kaplan–Meier plots were generated by using R (4.1.3) software (supplementary R code 12.2 and 12.3).

2.5. The enrichment analysis of gene set and the differentially expressed analysis of genes

To explore the GO immunity associated signaling pathways, we used the package clusterProfiler to analyze gene set enrichment (GSEA) [50] with the parameters below: p value-cutoff = 0.05 and q-value-cutoff = 0.05. The top forty terms of GO pathways were

shown. GO pathways with significant enrichment results were demonstrated based on gene ratio and P adjusted value. We considered Gene sets were remarkably enriched when $\text{padj} < 0.05$ [51] (supplementary R code 12.4).

The differentially expressed genes between two clusters were analyzed through R software package DESeq2 [52] (supplementary R code 5.1.1). $|\log_2\text{FoldChange}| > 1$ and adjusted $p < 0.05$ were the threshold values. We used the “ggpubr” and “ggthemes” packages to display differentially expressed genes in the volcano plots (supplementary R code 5.1.2).

2.6. Weighted gene coexpression network analysis

On the basis of differentially expressed genes we performed WGCNA through the R package [53]. In order to guarantee that the created coexpression network is close to scale-free distribution, 4 was chosen as the soft power. Then, we got four modules and their association with clusters, Stromal Score, Immune Score, ESTIMATE Score, and Tumor Purity were calculated. Then the genes were

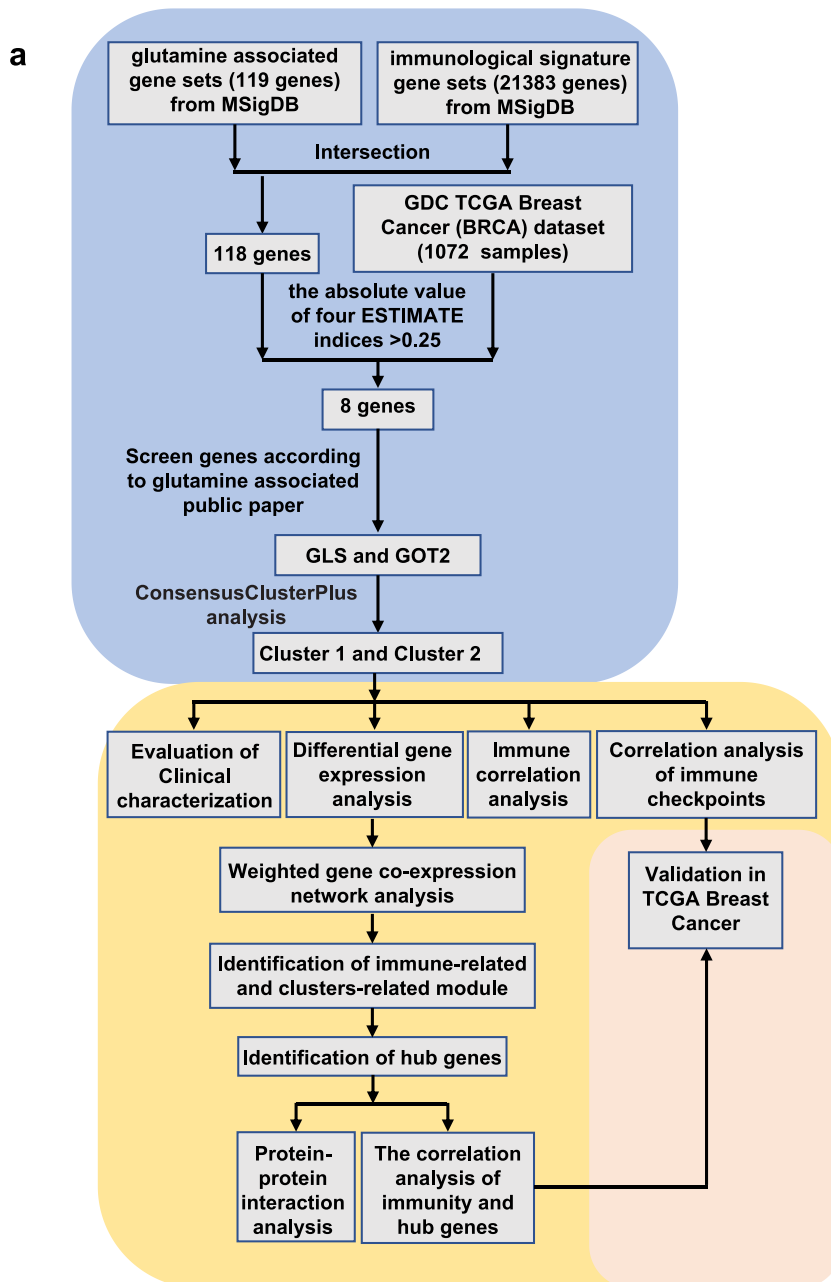


Fig. 1. The study design. (a) Workflow of data processing and bioinformatics analysis, comprising three main modules, including gene screening and consensus clustering, weighted gene coexpression network analysis and analysis of immune infiltration, and external validation.

obtained based on the values of module membership (MM) and gene significance (GS) ($MM > 0.40$ and $GS > 0.30$) (supplementary R code 5.2).

2.7. Gene–Gene and Gene–ESTIMATE interaction relationships

We used a search tool to retrieve interacting genes to evaluate the interaction between hub genes (STRING, <https://cn.string-db.org/>) [54] and established profiles of protein–protein interactions (supplementary R code 5.6). Spearman’s correlations of gene–gene and gene–ESTIMATE were analyzed through R package corplot (supplementary R code 5.4 and 5.5).

2.8. Statistical analysis

R (4.1.3) and SPSS (18.0) software were used to perform statistical analysis. And the Wilcoxon rank sum test was applied to perform

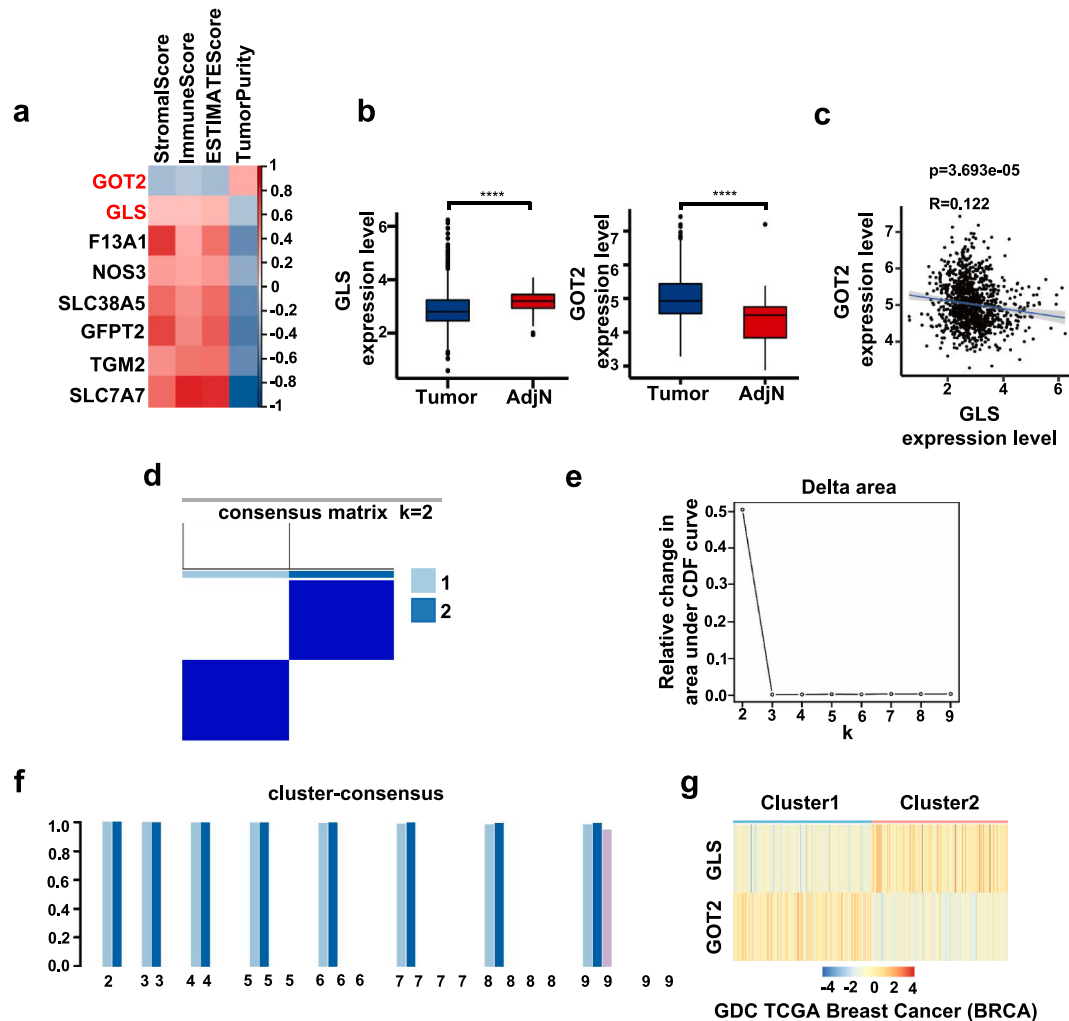


Fig. 2. Consensus clustering of breast cancer samples on the basis of GLS and GOT2 expression. (a) ESTIMATE analysis of immune- and glutamine-associated regulators. The absolute value of four ESTIMATE indices (Stromal Score, Immune Score, ESTIMATE Score and Tumor Purity) > 0.250 . Among them, red represented positive association, blue represented negative association, the darker the color, the stronger the association. (b) The expression of GLS and GOT2 in tumor and adjacent normal tissues. Red represents AdjN, blue represents tumor. **** $p < 0.001$. (c) The expression correlation analysis of GLS and GOT2. The expression of GLS was negative correlation with GOT2. $R = 0.122$, $p = 3.693e-05$. (d) Consistency matrix heat map was shown through consistency clustering ($k = 2$). Among them, light blue on behalf of Cluster 1, dark blue on behalf of Cluster 2. (e) The delta area helps to identification the most optimal number of clusters, which was $k = 2$. (f) Consistency score bar graph for subgroups with cluster counts between 2 and 9, and the optimal cluster counts was 2. Each colour represents a cluster, when the number of clusters is too large, and the number of patients in some clusters is too small, resulting in the disappearance of its colour block. (g) The GDC TCGA Breast Cancer (BRCA) dataset was divided into two clusters according to the expression of GLS and GOT2. The heatmap shows that GLS expressed lower and GOT2 expressed higher in Cluster 1 ($n = 541$), while GLS expressed higher and GOT2 expressed lower in Cluster 2 ($n = 531$).

the box plot analysis. We used Spearman's coefficient to perform the correlation analysis. The chi-square test was applied to weigh the clinical features between two clusters (the Fisher's exact test also was used when it was necessary). Multivariate logistic regression analysis was performed to estimate the clinical features between the clusters. Kaplan–Meier method (log-rank test) was performed to map survival curves. All hypothetical tests used in this study were two-sided, and the p value < 0.05 was significant.

3. Results

3.1. Consensus clustering based on the expression of GLS and GOT2 in breast cancer

The study design is shown in Fig. 1a. To investigate the roles of glutamine metabolism in the tumor immune microenvironment of breast cancer, all immunity-associated gene sets (including 21,383 genes) and glutamine-associated gene sets (including 119 genes) from the Molecular Signatures Database (MSigDB) were intersected, and we obtained 118 genes. By calculating four ESTIMATE indices, we found that 8 genes (including GOT2, GLS, F13A1, NOS3, SLC38A5, GFPT2, TGM2 and SLC7A7) were significantly associated with Stromal Score, Immune Score, ESTIMATE Score and Tumor Purity (Fig. 2a). There was not glutamine metabolism related reports about F13A1, NOS3, GFPT2, TGM2 and SLC7A7 genes. SLC38A5 is reported as a amino acid transporter shuttled amino acids (including glutamine) across cell member but not the glutamine specific transporter [55–57]. Both GLS and GOT2 were essential genes to glutamine metabolism [28,36,37]. GLS is the opening enzyme of glutamine metabolism, which converts glutamine to glutamate [28]. In addition, GOT2 inhibits glutamine metabolism in tumor [36]. So we using GLS and GOT2 for further analysis. GLS was positively associated with Stromal Score, Immune Score, ESTIMATE Score and negatively associated with Tumor Purity, and GOT2 was negatively associated with Stromal Score, Immune Score, ESTIMATE Score and positively associated with Tumor Purity (Fig. 2a). Then we analyzed the transcription levels of GLS and GOT2 in the GDC TCGA Breast Cancer (BRCA) dataset (n = 1072) through the Wilcoxon rank-sum test. Compared with tumor-adjacent tissue samples (AdjN), GLS expression level was decreased and GOT2 expression level was increased in breast tumor samples (Tumor) (Fig. 2b). Spearman's correlation analysis showed a negative correlation between GLS and GOT2 expression (R = 0.122, p = 3.693e-05) (Fig. 2c). Then, consensus analysis was performed to cluster the GDC TCGA Breast Cancer (BRCA) dataset according to the expression matrix of GLS and GOT2 through the ConsensusClusterPlus method. The classification of the two-subgroup was that the cluster consistency score of each subgroup is higher than 0.800 (Fig. 2d–f), suggesting that two group clustering was more reliable than multi-group clustering. The patterns of gene expression of Cluster 1 and Cluster 2 were significantly different, but the gene expression profiles within each cluster had high similarity (Fig. 2d and g). The 1072 breast cancer samples were divided into two clusters: Cluster 1 (GLS expressed lower and GOT2 expressed higher, n = 541) and Cluster 2 (GLS expressed higher and GOT2 expressed lower, n = 531) (Fig. 2g). These results suggest that the glutamine regulators GLS and GOT2 show opposite expression patterns in breast cancer, and the breast cancer samples can be divided into two clusters based on GLS and GOT2 expression patterns.

3.2. Evaluation of clinical characteristics

To better clarify the clinical properties of the clusters, we investigated the proportion of Cluster 1 and Cluster 2 in various molecular subtypes of breast cancer in the GDC TCGA Breast Cancer (BRCA) dataset. Cluster 2 was the predominant cluster in the subtype of TNBC (Supplementary Fig. S1a). We also observed that in luminal B subtype, the share of Cluster 1 was slightly larger than that of

Table 1
Clinical features of the two clusters.

	Cluster1	Cluster2	P value
n	451	447	
age (mean)	59.984	55.470	<0.001
gender = male (%)	8 (1.774)	3 (0.671)	0.231
pathological.stage(%)			0.244
Stage 1	75 (16.630)	80 (17.897)	
Stage 2	254 (56.319)	272 (60.850)	
Stage 3	112 (24.834)	88 (19.687)	
Stage 4	10 (2.217)	7 (1.566)	
T.stage(%)			0.031
T1	105 (23.282)	126 (28.188)	
T2	271 (60.089)	262 (58.613)	
T3	51 (11.308)	50 (11.186)	
T4	24 (5.321)	9 (2.013)	
N.stage(%)			0.421
N0	213 (47.228)	231 (51.678)	
N1	160 (35.477)	137 (30.649)	
N2	49 (10.865)	53 (11.856)	
N3	29 (6.430)	26 (5.817)	
M.stage(%)			0.638
M0	441 (97.783)	440 (98.434)	
M1	10 (2.217)	7 (1.566)	

Cluster 2 (Supplementary Fig. S1a), and the proportions of Cluster 1 and Cluster 2 were no significant difference between the HER2-enriched and luminal A subtypes (Supplementary Fig. S1a). These data suggest that Cluster 2 had a latent correlation with the TNBC subtype in breast cancer.

We also analyzed the survival rate in the GDC TCGA Breast Cancer (BRCA) dataset. However, the survival rates were not significantly different between the Cluster 1 and Cluster 2 in TNBC (Supplementary Fig. S2a), HER2-enriched (Supplementary Fig. S2b), luminal A (Supplementary Fig. S2c) and luminal B (Supplementary Fig. S2d) subtypes of breast cancer. The correlation analysis showed that the T stage and age correlation degree in Cluster 1 were higher comparing with Cluster 2 (Table 1). In addition, multivariate logistic regression analysis showed that the independent factors were T stage, N stage, age and pathological stage, which affecting clustering (Table 2). The above data indicate that the clusters are related with the prognosis of breast cancer.

3.3. Cluster 2 is related to dendritic cells in breast cancer

We further analyzed the immune infiltration in Cluster 1 and Cluster 2. We performed ESTIMATE analysis to evaluate the immune association in Cluster 1 and Cluster 2. We found that the Stromal Score, Immune Score and ESTIMATE Score of Cluster 2 were higher compared with Cluster1, and the Tumor Purity was lower than that of Cluster 1 (Fig. 3a). The expressed extent of genes about Cluster 1 and Cluster 2 were compared, and GSEA analysis was performed using the differentially expressed genes. We found many immunity-associated pathways among the top 40 pathways (Supplementary Fig. S3a). We also performed CIBERSORT and ssGSEA analysis to explore the differences of the immunity functions between the Cluster 1 and Cluster 2. CIBERSORT analysis revealed that Cluster 2 had a higher proportion of dendritic cells and M1 macrophages, and a lower proportion of CD4 memory T cells, follicular helper T cells and CD8 T cells comparing with Cluster 1 (Fig. 3b). Consistent with CIBERSORT analysis, ssGSEA also showed that there was a higher infiltration extent of dendritic cells in Cluster 2 than Cluster 1 (Fig. 3c).

To further explore the association between immune infiltration and clusters, we analyzed the transcription level in the GDC TCGA Breast Cancer (BRCA) dataset. Comparing Cluster 2 with Cluster 1, we got 1073 up-regulated genes and 397 down-regulated genes in the volcano plot (Fig. 4a). The expression profiles of differential genes were used for further WGCNA, and we identified 4 modules (Fig. 4b and c). The blue module was positively associated with Cluster (R = 0.390, p = 8.000e-41), StromalScore (R = 0.370, p = 7.000e-37), ImmuneScore (R = 0.870, p = 0.000), and ESTIMATEScore (R = 0.730, p = 4.000e-180) and negatively associated with TumorPurity (R = -0.760, P = 1.000e-203) (Fig. 4d). From the blue module, we identified 71 hub genes based on MM > 0.400 and GS > 0.300 (Fig. 4e). Among these genes, we found that 11 genes (VCAM1 [58], PTPN22 [59], ICAM1 [60], IL7R [61], TNFSF14 [62], GPR174 [63], CCR2 [64], CCR4 [65], CTLA4 [66], LYN [67–69] and RUNX3 [70]) were essential for dendritic cell development, maturation, activation and other functions. Spearman's correlation analysis between genes and ESTIMATE analysis also showed that these dendritic cell-associated genes were positive associated with ESTIMATE Score and were negative associated with Tumor Purity (Fig. 4f). The gene expression correlation analysis also showed that these genes were positive correlation with GLS expression and were negative correlation with GOT2 expression (Fig. 4g). The protein–protein interaction analysis showed that 10 dendritic cell-associated genes, VCAM1, PTPN22, ICAM1, IL7R, GPR174, CCR2, CCR4, CTLA4, LYN and RUNX3, were correlated (Fig. 4h). Thus, all these results demonstrated that Cluster 2 was positive association with dendritic cells in breast cancer.

3.4. The better response to immunotherapy in cluster 2 than cluster 1

The expression level of these immune checkpoint genes is critical for the immune checkpoint therapeutic strategy [23], which is another promising means for immunotherapy [21]. In addition to its dendritic cell-associated function, CTLA4 is also an immune checkpoint gene. We also observed that the CTLA4 gene showed a higher expression level in Cluster 2 than in Cluster 1. Thus, we compared immune checkpoint gene expression extent in these two clusters. We observed that the expression level of PD1-related genes (PD1, PDL1 and PDL2) (Fig. 5a), CTLA4-related genes (CD80, CD86 and CTLA4) (Fig. 5b), other immune checkpoint genes (LAG3,

Table 2
Multivariate logistic regression for clustering (Cluster 2 vs Cluster 1).

Variables	Multivariate Logistic Regression	
	Odds Ratio (95% Confidence Interval)	P value
age	0.969 (0.959–0.980)	0.0001
T stage		0.032
T2 vs T1	2.155 (0.722–6.435)	0.169
T3 vs T1	1.111 (0.420–2.939)	0.832
T4 vs T1	1.752 (0.677–4.534)	0.248
N stage		0.004
N1 vs N0	0.410 (0.164–1.024)	0.056
N2 vs N0	0.299 (0.128–0.700)	0.005
N3 vs N0	1.072 (0.536–2.141)	0.845
Pathological stage		0.003
stage2 vs stage1	1.366 (0.316–5.893)	0.676
stage3 vs stage1	2.598 (0.736–9.171)	0.138
stage4 vs stage1	0.758 (0.259–2.219)	0.613

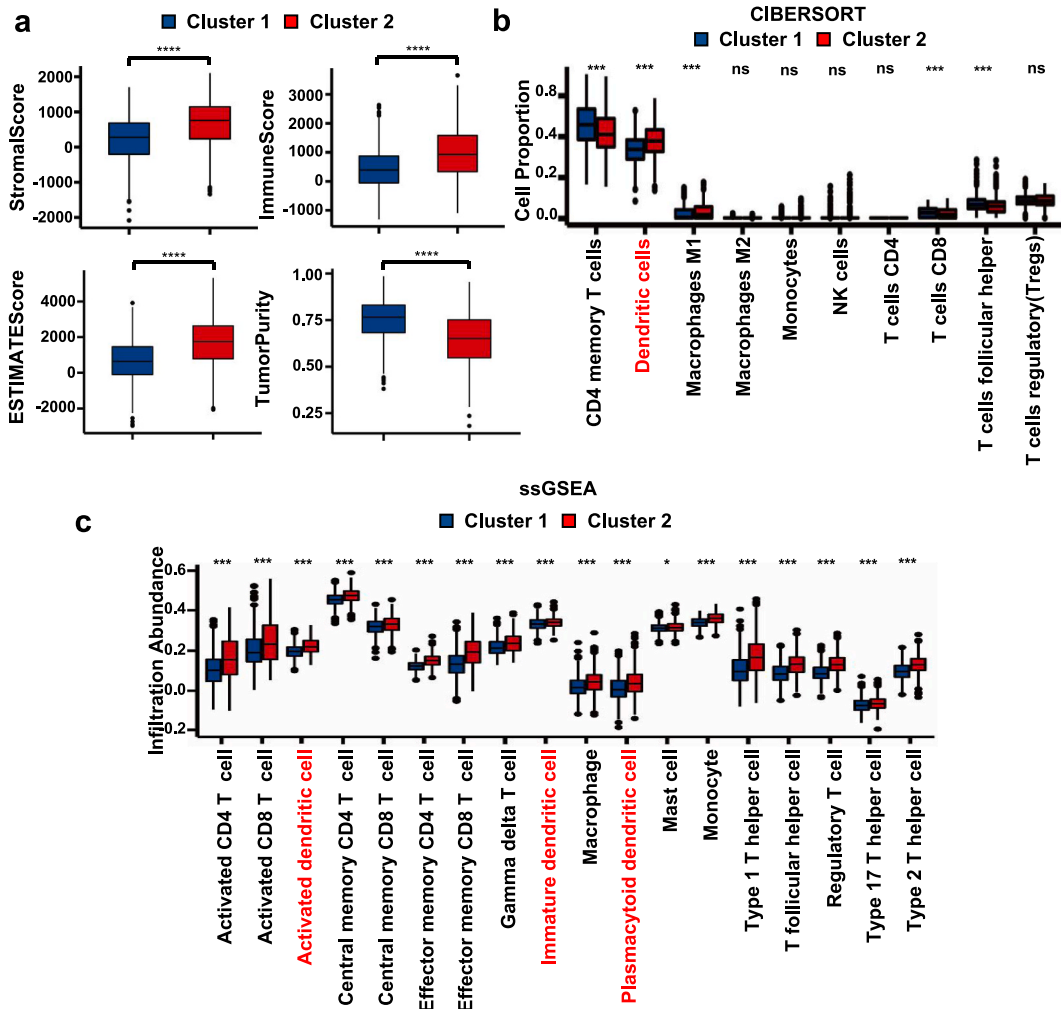


Fig. 3. Comparing the characteristics of Immune Infiltration between the Cluster 1 and Cluster 2. (a) ESTIMATE analysis in Cluster 1 and Cluster 2. The Stromal Score, Immune Score and ESTIMATE Score of Cluster 2 were higher, and the tumor purity was lower comparing with Cluster 1. (b) CIBERSORT analysis revealed that the portion of dendritic cells in Cluster 2 was larger compared that with Cluster 1. (c) ssGSEA revealed that Cluster 2 showed a higher infiltration extent of dendritic cells compared with Cluster 1. Red represented Cluster 2, blue represented Cluster 1. ns, no significance, * $p < 0.05$, *** $p < 0.005$, and **** $p < 0.001$.

TIGIT and TIM3) (Fig. 5c), and agonists of T-cell activation genes (4-1BB, CD27, CD40, CD70, ICOS and OX40) (Fig. 5d) were significant higher in Cluster 2 than Cluster 1. These results suggested that the immunotherapy responses in Cluster 2 was better than in Cluster 1.

3.5. Validation of immune characteristics between the cluster 1 and cluster 2

To validate the immune characteristics between the Cluster 1 and Cluster 2, we used the TCGA Breast Cancer (BRCA) dataset ($n = 1097$) for further analysis. We used the same method which previously performed in the validation dataset to divided the breast cancer samples into two clusters. Consistent with the GDC TCGA Breast Cancer (BRCA) dataset, the cluster consistency scores of each subgroup were higher than 0.8 (Fig. 6a–c), suggesting that it was more reliable to divide into two groups than divide into more groups in the validation dataset. The gene expression profiles of Cluster 1 and Cluster 2 were also significantly different, but the gene expression profiles within each cluster had high similarity (Fig. 6a and d). GLS expressed lower and GOT2 expressed higher in Cluster 1 ($n = 558$), while the GLS expressed higher and GOT2 expressed lower in Cluster 2 ($n = 539$) in the validation dataset (Fig. 6d).

We also performed ESTIMATE analysis to evaluate the immune features in Cluster 1 and Cluster 2 of the verification dataset. We found the Stromal Score, Immune Score and ESTIMATE Score of the Cluster 2 were higher compared those with Cluster 1, and the tumor purity was lower than that of Cluster 1 (Fig. 7a). Both CIBERSORT and ssGSEA revealed that Cluster 2 was positive association with dendritic cells compared with Cluster 1 in the validation dataset (Fig. 7b and c). The expression of 11 dendritic cell-associated genes (VCAM1, PTPN22, ICAM1, IL7R, TNFSF14, GPR174, CCR2, CCR4, CTLA4, LYN and RUNX3) identified in Fig. 4 was also

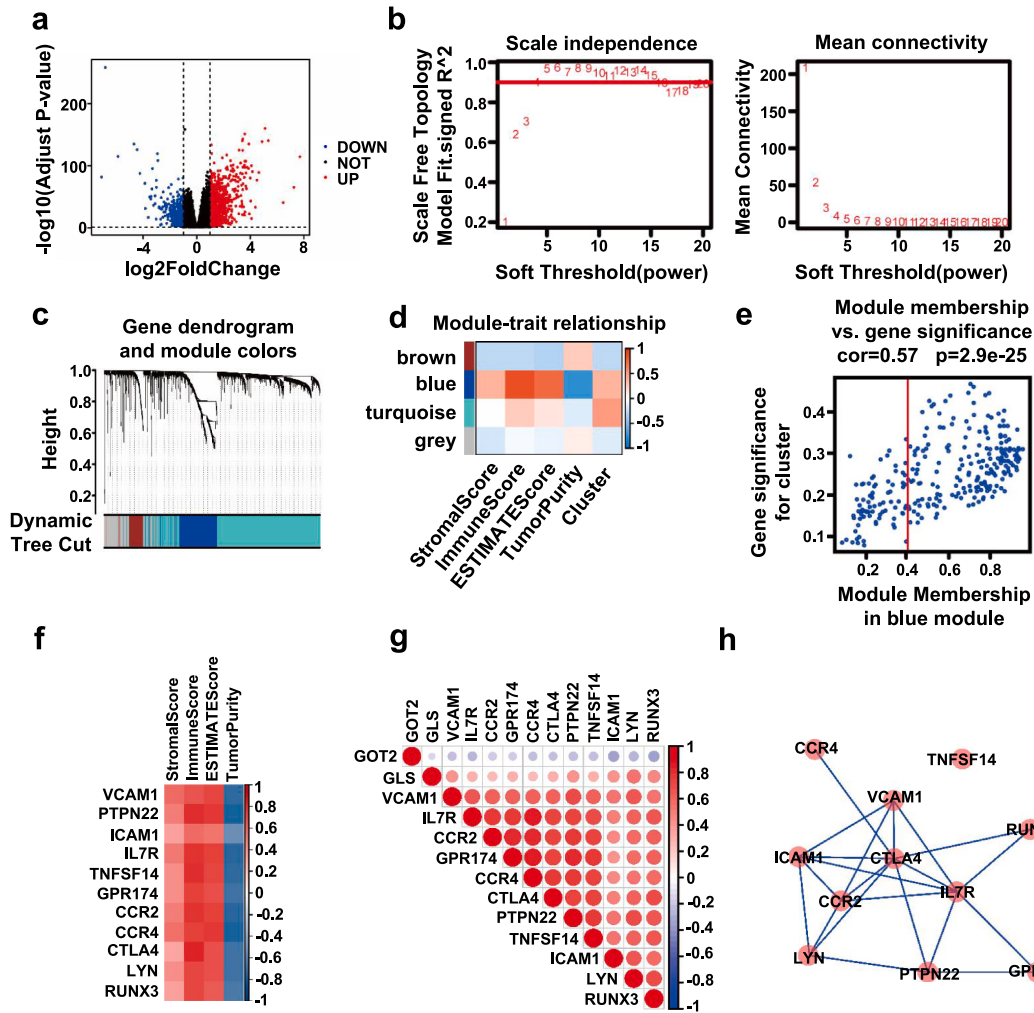


Fig. 4. Cluster 2 positively correlated with dendritic cell maturation-associated genes. (a) Volcano diagram showed the differential gene expression analysis between the Cluster 2 and Cluster 1. Red represented upregulated genes, blue represented downregulated genes, and black represented no change in genes comparing Cluster 2 with Cluster 1. (b) Network topology analysis of soft power (soft powers = 4). (c) Gene dendrogram and module colours. (d) Heatmap among module eigengenes, Cluster and ESTIMATE results. We identified a module (blue) correlated with glutamine metabolism (Cluster, $R = 0.390$, $p = 8.000e-41$) and immunity (Immune Score, $R = 0.870$, $p = 0.000$) (e) Scatter diagram of module eigengenes in the blue module ($MM > 0.400$ and $GS > 0.300$), and through it we found 71 hub genes. (f) Relevance between hub genes (11 genes which among hub genes were essential for dendritic cell development, maturation, activation and other functions.) and results of four ESTIMATE indices (Stromal Score, Immune Score, ESTIMATE Score and Tumor Purity). Red represented positive association, blue represented negative association, and the darker the color, the stronger the connection. (g) Association between the expression of 11 hub genes and GLS or GOT2. Red represented positive correlation, blue represented negative correlation. The darker the colour, the stronger the correlation. (h) Protein-protein interaction network of 11 hub genes.

positive correlation with GLS and negative correlation with GOT2 in the validation dataset (Fig. 8a). Spearman's correlation analysis between genes and four ESTIMATE indices also showed that these genes were positive associated with ESTIMATE Score and negative associated with Tumor Purity (Fig. 8b). Above studies demonstrated that Cluster 2 was positive association with dendritic cells in the validation dataset.

We also observed that the expression level of the immune checkpoint genes: PD1-related genes (PD1, PDL1, PDL2) (Fig. 9a), CTLA4-related genes (CD80, CD86, CTLA4) (Fig. 9b), other immune checkpoint genes (LAG3, TIGIT, TIM3) (Fig. 9c), and agonists of T-cell activation genes (4-1BB, CD27, CD40, CD70, ICOS and OX40) (Fig. 9d) were also higher in Cluster 2 compared with those in Cluster 1 of the validation dataset. These results suggest that the immunotherapy response of Cluster 2 was better than Cluster 1 in the validation dataset.

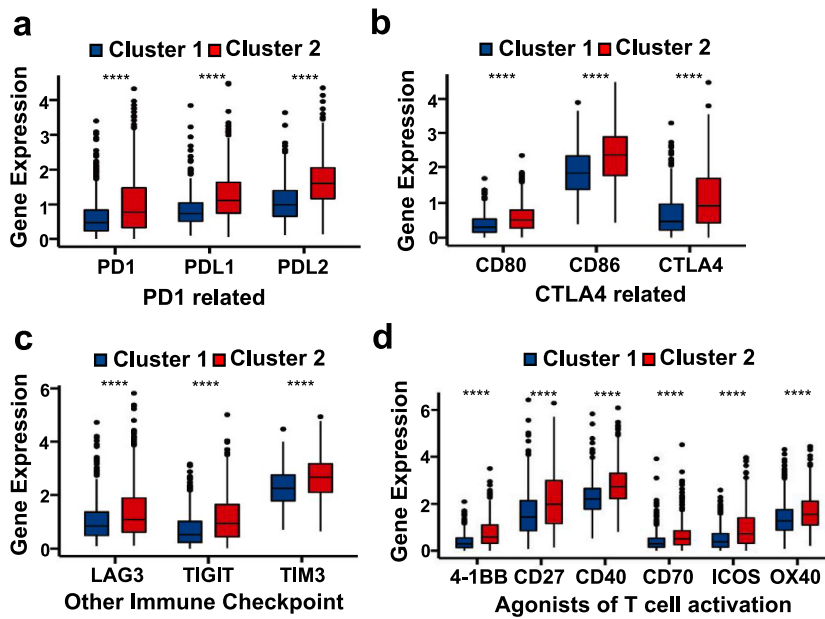


Fig. 5. Comparison of the expression of immune checkpoint gene between the Cluster 1 and Cluster 2. Comparing the expression of PD1-related genes (a), CTLA4-related genes (b), other immune checkpoint genes (c) and agonists of T-cell activation genes (d) between the Cluster 1 and Cluster 2. Red represented Cluster 2, blue represents Cluster 1. **** $p < 0.001$.

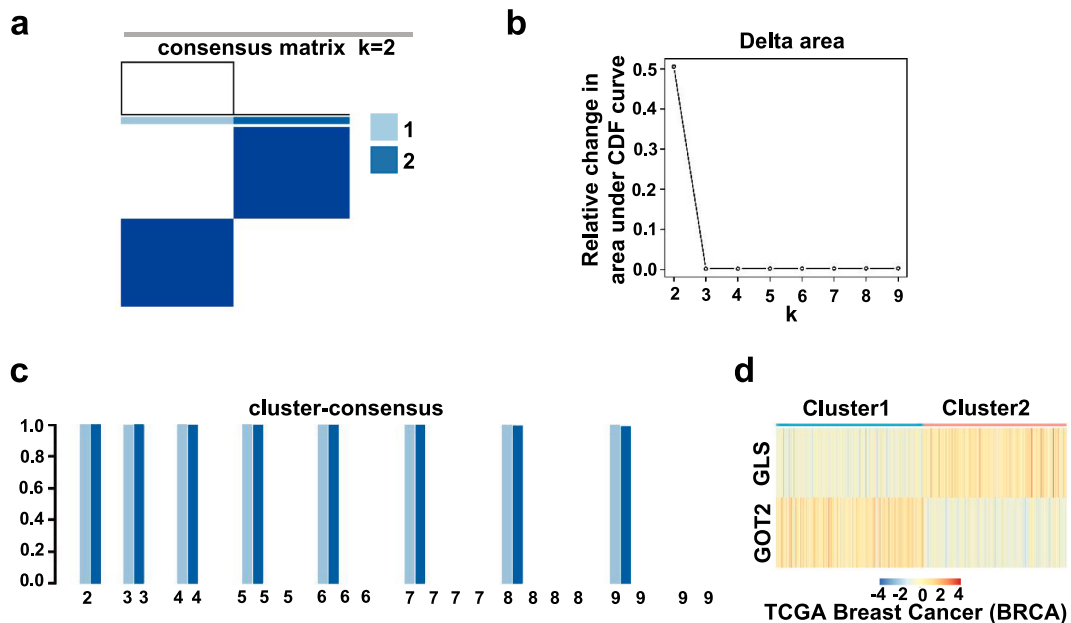


Fig. 6. Validation of clustering in the GDC TCGA Breast Cancer (BRCA) dataset. (a) Heatmap corresponding to consensus matrix using consensus clustering ($k = 2$). Among them, light blue represented Cluster 1, dark blue represented Cluster 2. (b) The delta area helps to make sure the most optimal number of clusters. (c) Consensus score bar graph for subgroups with cluster counts ranging from 2 to 9, and the optimal cluster counts was 2. Each colour represents a cluster, when the number of clusters is too large, and the number of patients in some clusters is too small, resulting in the disappearance of its colour block. (d) The validation dataset was divided into two clusters according to the expression of GLS and GOT2. The heatmap shows that GLS expressed low and GOT2 expressed high in Cluster 1 ($n = 558$), while GLS expressed high and GOT2 expressed low in Cluster 2 ($n = 539$).

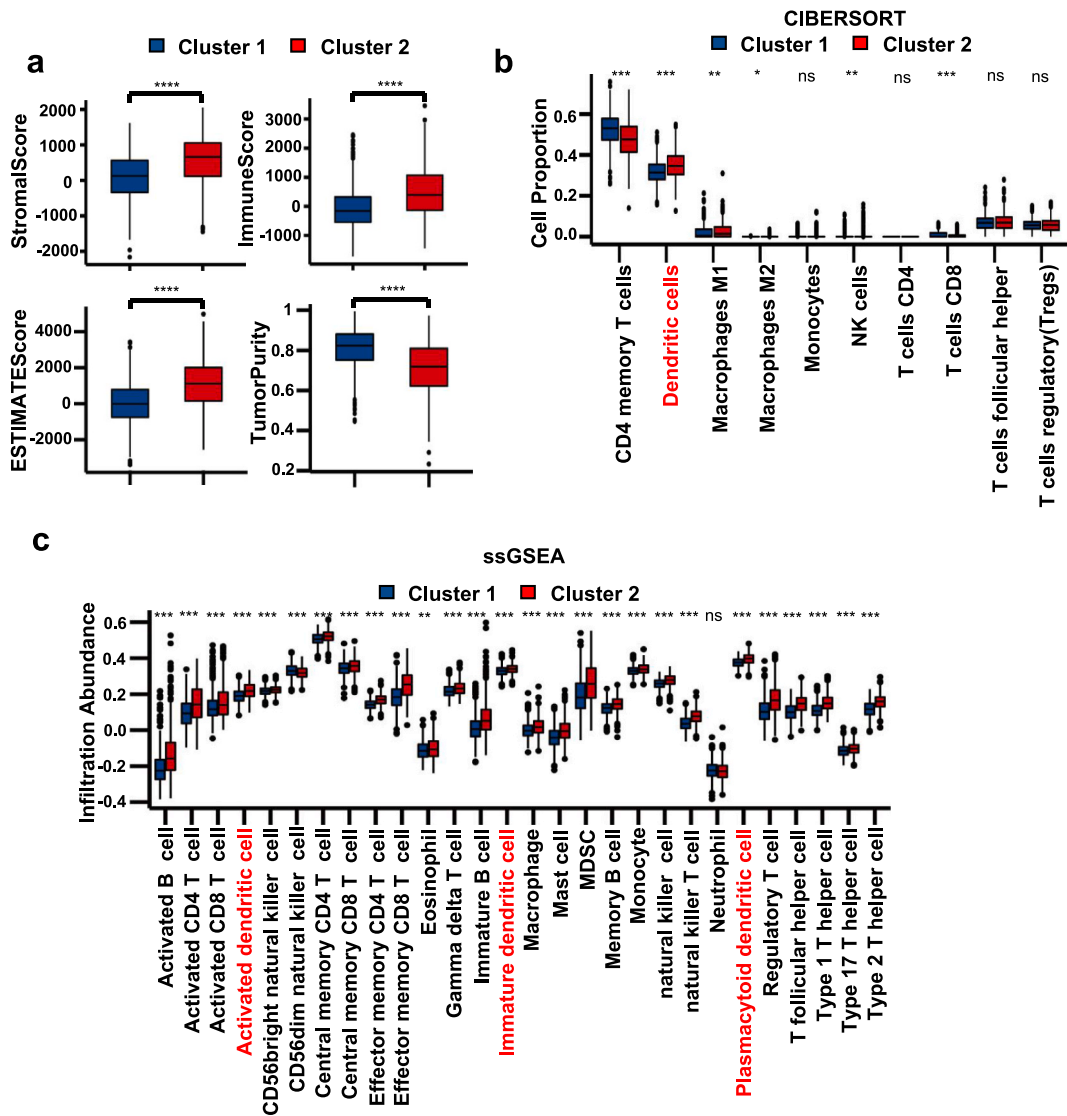


Fig. 7. Validation of Characteristics of Immunity between the Cluster 1 and Cluster 2. (a) ESTIMATE analysis in Cluster 1 and Cluster 2. The Stromal Score, Immune Score and ESTIMATE Score of Cluster 2 were higher, and the tumor purity was lower compared with Cluster 1. (b) CIBERSORT analysis revealed that the portion of dendritic cells in Cluster 2 was larger compared with that in Cluster 1. (c) ssGSEA revealed that Cluster 2 showed a larger infiltration extent of dendritic cells compared with Cluster 1. Red represented Cluster 2, blue represented Cluster 1. ns, no significance, * $p < 0.05$, ** $p < 0.01$, *** $p < 0.005$, and **** $p < 0.001$.

4. Conclusions and discussion

Altogether, our study indicates that GLS and GOT2 are prognostic biomarkers associated with dendritic cells and response to immunotherapy in breast cancer.

GLS and GOT2 are associated with T cells and the microenvironment of immunity in cancer [34,35,38,39,71]. GLS is positively associated with the extent of immune infiltration in cancer [34]. In the microenvironment of tumor immunity, GLS is positive correlation with resting memory CD4 T cells and negative correlation with monocytes [35]. Inhibiting GLS in cancer cells can diminish tumor immune evasion [33] and enhance the antimelanoma activity of T-cell-mediated immunotherapies [71]. GOT2 suppresses antitumor immunity through spatial limitation of both CD4⁺ and CD8⁺ T cells [38]. High GOT2 expression is positive association with the immunologically quiet subtype of clear-cell renal cell carcinoma [39]. In our study, however, we found an association between dendritic cells and the expression level of GLS and GOT2 in breast cancer. And divided breast cancer patients into two clusters on the basis of the expression of GLS and GOT2: Cluster 1 (GLS low expressed and GOT2 high expressed) and Cluster 2 (GLS high expressed and GOT2 low expressed). Cluster 2 (GLS expressed high and GOT2 expressed low) breast cancer showed a higher association with dendritic cells, implying that GLS and GOT2 may also be involved in dendritic cell regulation. Further gene expression correlation

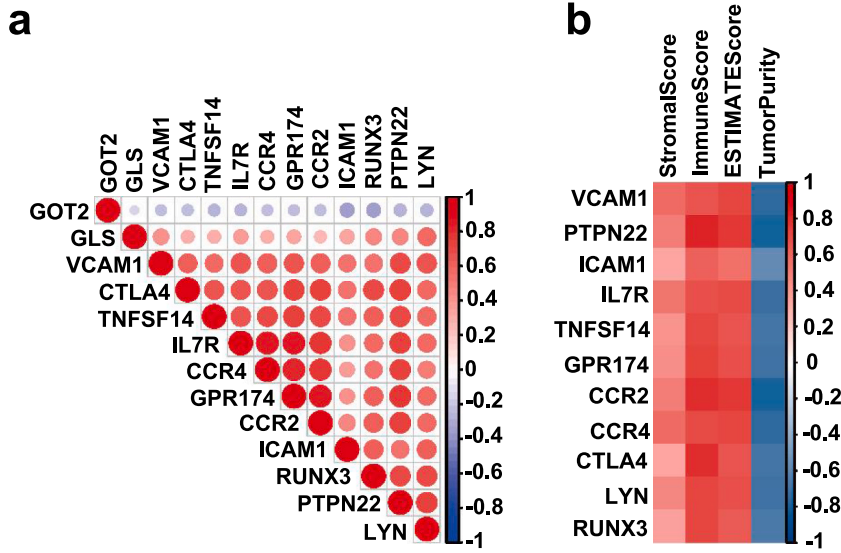


Fig. 8. Dendritic cell-associated gene expression analysis in the validation dataset. (a) Association between the expression of dendritic cell-associated genes and GLS or GOT2. (b) Association between hub genes and the ESTIMATE indice (Stromal Score, Immune Score, ESTIMATE Score or Tumor Purity). Red represented positive correlation, blue represented negative correlation. The darker the colour, the stronger the correlation.

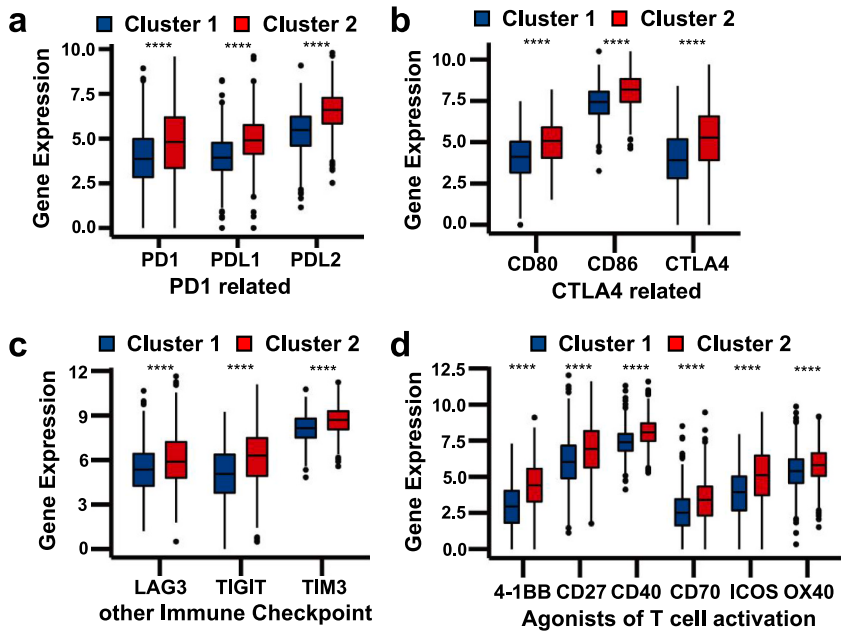


Fig. 9. Comparison of the expression of immune checkpoint gene between the Cluster 1 and Cluster 2 in the validation dataset. Comparison of PD1-related genes (a), CTLA4-related genes (b), other immune checkpoint genes (c) and agonists of T-cell activation genes (d) between the Cluster 1 and Cluster 2. Red represented Cluster 2, blue represents Cluster 1. ****p < 0.001.

analysis found dendritic cell-associated genes (VCAM1 [58], PTPN22 [59], ICAM1 [60], IL7R [61], TNFSF14 [62], GPR174 [63], CCR2 [64], CCR4 [65], CTLA4 [66], LYN [67–69] and RUNX3 [70]), suggesting that glutamine metabolism regulated by GLS and GOT2 may play important roles in dendritic cell development maturation, activation and other functions of dendritic cells. The association between the expressions of GLS and GOT2 and dendritic cells may provide a new clue regarding how glutamine metabolism regulates antitumor immunity. The mechanism by which GLS and GOT2 regulate dendritic cell maturation awaits discovery.

Targeting immune checkpoint pathways is a promising means for cancer immunotherapy [21]. In our study, we found that Cluster 2 (GLS expressed high and GOT2 expressed low) was positively associated with immune checkpoint gene expression, implying that GLS and GOT2 may be involved in immune checkpoint pathway regulation. These results indicated that the immunotherapy response of

Cluster 2 is better. Therefore, this classification based on GLS and GOT2 expression may provide guidance for breast cancer immunotherapy. The mechanism by which GLS and GOT2 regulate the immune checkpoint pathway needs to be further explored.

The normal breast tissues have a large number of immune cell population, including CD8⁺ and CD4⁺ T cells, B cells, dendritic cells, macrophages, NK cells, and other immune cell subtypes, which constitute the immune microenvironment and eliminate transformed breast cells [45,72,73]. TNBC which is lack of the expression of ER, PR, and HER2, is related to a low overall survival rate and a high recurrence rate [74–76]. In our study, we observed that Cluster 2 (GLS expressed high and GOT2 expressed low) was predominantly in the TNBC subtype, implying that the GLS and GOT2 genes may be considered as immunotherapy biomarkers for the TNBC subtype. The mechanism of GLS and GOT2 regulate the microenvironment of immunity and immune checkpoint pathway can provide new clues for TNBC treatment.

Data availability statement

The datasets used in the manuscript were from TCGA dataset (dataset ID: TCGA-BRCA.htseq_fpkms.tsv and TCGA.BRCA.sample-Map/HiSeqV2) and GEO dataset (GSE114725). The data included in supplementary material in the article or will be made available on request.

Funding disclosure

This study was supported by grants from the National Natural Science Foundation of China (82173044).

Ethics declarations

Review and approval by an ethics committee and informed consent were not required for this study because the dataset we used were download from the TCGA dataset.

CRediT authorship contribution statement

Ruifang Yang: Writing - original draft, Project administration, Investigation. **Shuo Cheng:** Project administration. **Jie Xiao:** Data curation. **Yujie Pei:** Investigation. **Zhonglin Zhu:** Investigation. **Jifa Zhang:** Project administration. **Jing Feng:** Project administration. **Jing Li:** Writing - review & editing, Writing - original draft.

Declaration of competing interest

The authors declare the following financial interests/personal relationships which may be considered as potential competing interests: Jing Feng reports financial support was provided by National Natural Science Foundation of China. If there are other authors, they declare that they have no known competing financial interests or personal relationships that could have appeared to influence the work reported in this paper.

Acknowledgments

The authors sincerely thank all the participated staff in this study and all the publicly available data used in this study. Thanks for the support of multifunctional platforms of innovation (011) of East China Normal University.

Appendix A. Supplementary data

Supplementary data to this article can be found online at <https://doi.org/10.1016/j.heliyon.2024.e24163>.

References

- [1] R.L. Siegel, et al., Cancer statistics, Ca - Cancer J. Clin. 72 (1) (2022) 7–33, 2022.
- [2] X. Dai, et al., Breast cancer intrinsic subtype classification, clinical use and future trends, Am. J. Cancer Res. 5 (10) (2015) 2929–2943.
- [3] J. Kufel-Grabowska, et al., Fertility counseling in BRCA1/2-mutated women with breast cancer and healthy individuals, J. Clin. Med. 11 (14) (2022).
- [4] J. Maksimenko, A. Irmejs, J. Gardovskis, Pregnancy after breast cancer in BRCA1/2 mutation carriers, Hered. Cancer Clin. Pract. 20 (1) (2022) 3.
- [5] J. Rosin, et al., Discordance of PIK3CA Mutational Status between Primary and Metastatic Breast Cancer: a Systematic Review and Meta-Analysis, Breast Cancer Res Treat, 2023.
- [6] K. Kawaguchi, Y. Maeshima, M. Toi, Tumor immune microenvironment and systemic response in breast cancer, Med. Oncol. 39 (12) (2022) 208.
- [7] A. Arab, R. Yazdian-Robati, J. Behravan, HER2-Positive breast cancer immunotherapy: a focus on vaccine development, Arch. Immunol. Ther. Exp. 68 (1) (2020) 2.
- [8] E. Krasniqi, et al., Immunotherapy in HER2-positive breast cancer: state of the art and future perspectives, J. Hematol. Oncol. 12 (1) (2019) 111.
- [9] Y. Tokumaru, D. Joyce, K. Takabe, Current status and limitations of immunotherapy for breast cancer, Surgery 167 (3) (2020) 628–630.
- [10] D. Stevens, et al., Dendritic cell-based immunotherapy in lung cancer, Front. Immunol. 11 (2020) 620374.

- [11] J. Banchereau, R.M. Steinman, Dendritic cells and the control of immunity, *Nature* 392 (6673) (1998) 245–252.
- [12] R.M. Steinman, J. Banchereau, Taking dendritic cells into medicine, *Nature* 449 (7161) (2007) 419–426.
- [13] R.M. Steinman, Decisions about dendritic cells: past, present, and future, *Annu. Rev. Immunol.* 30 (2012) 1–22.
- [14] G. Jego, et al., Dendritic cells control B cell growth and differentiation, *Curr. Dir. Autoimmun.* 8 (2005) 124–139.
- [15] H. Qi, et al., Extrafollicular activation of lymph node B cells by antigen-bearing dendritic cells, *Science* 312 (5780) (2006) 1672–1676.
- [16] B.C. Gil-Torregrosa, et al., Control of cross-presentation during dendritic cell maturation, *Eur. J. Immunol.* 34 (2) (2004) 398–407.
- [17] F. Granucci, et al., Early events in dendritic cell maturation induced by LPS, *Microb. Infect.* 1 (13) (1999) 1079–1084.
- [18] C. Reis e Sousa, Dendritic cells in a mature age, *Nat. Rev. Immunol.* 6 (6) (2006) 476–483.
- [19] P. Vargas, et al., Innate control of actin nucleation determines two distinct migration behaviours in dendritic cells, *Nat. Cell Biol.* 18 (1) (2016) 43–53.
- [20] G. Faure-André, et al., Regulation of dendritic cell migration by CD74, the MHC class II-associated invariant chain, *Science* 322 (5908) (2008) 1705–1710.
- [21] B. Li, et al., Targeting glutaminase 1 attenuates stemness properties in hepatocellular carcinoma by increasing reactive oxygen species and suppressing Wnt/beta-catenin pathway, *EBioMedicine* 39 (2019) 239–254.
- [22] N. Gaynor, J. Crown, D.M. Collins, Immune checkpoint inhibitors: key trials and an emerging role in breast cancer, *Semin. Cancer Biol.* 79 (2022) 44–57.
- [23] X. He, C. Xu, Immune checkpoint signaling and cancer immunotherapy, *Cell Res.* 30 (8) (2020) 660–669.
- [24] T. Yang, et al., Meta-analysis of glutamine on immune function and post-operative complications of patients with colorectal cancer, *Front. Nutr.* 8 (2021) 765809.
- [25] S.J. Fan, et al., Glutamine deprivation alters the origin and function of cancer cell exosomes, *EMBO J.* 39 (16) (2020) e103009.
- [26] J.M. Carrascosa, P. Martínez, I. Núñez de Castro, Nitrogen movement between host and tumor in mice inoculated with Ehrlich ascitic tumor cells, *Cancer Res.* 44 (9) (1984) 3831–3835.
- [27] G. Ma, et al., Reprogramming of glutamine metabolism and its impact on immune response in the tumor microenvironment, *Cell Commun. Signal.* 20 (1) (2022) 114.
- [28] C.T. Hensley, A.T. Wasti, R.J. DeBerardinis, Glutamine and cancer: cell biology, physiology, and clinical opportunities, *J. Clin. Invest.* 123 (9) (2013) 3678–3684.
- [29] J. Zhang, et al., Inhibition of GLS suppresses proliferation and promotes apoptosis in prostate cancer, *Biosci. Rep.* 39 (6) (2019).
- [30] A. Mukha, et al., GLS-driven glutamine catabolism contributes to prostate cancer radiosensitivity by regulating the redox state, stemness and ATG5-mediated autophagy, *Theranostics* 11 (16) (2021) 7844–7868.
- [31] V.M. Ngwa, et al., Loss of vascular endothelial glutaminase inhibits tumor growth and metastasis, and increases sensitivity to chemotherapy, *Cancer Res. Commun.* 2 (7) (2022) 694–705.
- [32] Y. Xiang, et al., Targeted inhibition of tumor-specific glutaminase diminishes cell-autonomous tumorigenesis, *J. Clin. Invest.* 125 (6) (2015) 2293–2306.
- [33] J.A. Segura, et al., Ehrlich ascites tumor cells expressing anti-sense glutaminase mRNA lose their capacity to evade the mouse immune system, *Int. J. Cancer* 91 (3) (2001) 379–384.
- [34] Z. Ouyang, et al., Bioinformatic profiling identifies the glutaminase to be a potential novel cuproptosis-related biomarker for glioma, *Front. Cell Dev. Biol.* 10 (2022) 982439.
- [35] Z. Liu, et al., Identification of GLS as a cuproptosis-related diagnosis gene in acute myocardial infarction, *Front. Cardiovasc. Med.* 9 (2022) 1016081.
- [36] Y. Li, et al., GOT2 silencing promotes reprogramming of glutamine metabolism and sensitizes hepatocellular carcinoma to glutaminase inhibitors, *Cancer Res.* 82 (18) (2022) 3223–3235.
- [37] S. Yang, et al., Mitochondrial glutamine metabolism via GOT2 supports pancreatic cancer growth through senescence inhibition, *Cell Death Dis.* 9 (2) (2018) 55.
- [38] J. Abrego, et al., A cancer cell-intrinsic GOT2-PPAR δ Axis suppresses antitumor immunity, *Cancer Discov.* 12 (10) (2022) 2414–2433.
- [39] W.A.S. Ferreira, E.H.C. de Oliveira, Expression of GOT2 is epigenetically regulated by DNA methylation and correlates with immune infiltrates in clear-cell renal cell carcinoma, *Curr. Issues Mol. Biol.* 44 (6) (2022) 2472–2489.
- [40] A. Colaprico, et al., TCGAAbiolinks: an R/Bioconductor package for integrative analysis of TCGA data, *Nucleic Acids Res.* 44 (8) (2016) e71.
- [41] K. Yoshihara, et al., Inferring tumour purity and stromal and immune cell admixture from expression data, *Nat. Commun.* 4 (2013) 2612.
- [42] A.M. Newman, et al., Robust enumeration of cell subsets from tissue expression profiles, *Nat. Methods* 12 (5) (2015) 453–457.
- [43] A.M. Newman, et al., Determining cell type abundance and expression from bulk tissues with digital cytometry, *Nat. Biotechnol.* 37 (7) (2019) 773–782.
- [44] C.M. Mousset, et al., Comprehensive phenotyping of T cells using flow cytometry, *Cytometry* 95 (6) (2019) 647–654.
- [45] E. Azizi, et al., Single-cell map of diverse immune phenotypes in the breast tumor microenvironment, *Cell* 174 (5) (2018) 1293–1308.e36.
- [46] H.A. Pflner, J. Shendure, C. Trapnell, Supervised classification enables rapid annotation of cell atlases, *Nat. Methods* 16 (10) (2019) 983–986.
- [47] S. Hänzelmann, R. Castelo, J. Guinney, GSVA: gene set variation analysis for microarray and RNA-seq data, *BMC Bioinf.* 14 (2013) 7.
- [48] G. Bindea, et al., Spatiotemporal dynamics of intratumoral immune cells reveal the immune landscape in human cancer, *Immunity* 39 (4) (2013) 782–795.
- [49] M.D. Wilkerson, D.N. Hayes, ConsensusClusterPlus: a class discovery tool with confidence assessments and item tracking, *Bioinformatics* 26 (12) (2010) 1572–1573.
- [50] G. Yu, et al., clusterProfiler: an R package for comparing biological themes among gene clusters, *OMICS* 16 (5) (2012) 284–287.
- [51] A. Subramanian, et al., Gene set enrichment analysis: a knowledge-based approach for interpreting genome-wide expression profiles, *Proc. Natl. Acad. Sci. U.S.A.* 102 (43) (2005) 15545–15550.
- [52] M.I. Love, W. Huber, S. Anders, Moderated estimation of fold change and dispersion for RNA-seq data with DESeq2, *Genome Biol.* 15 (12) (2014) 550.
- [53] P. Langfelder, S. Horvath, WGCNA: an R package for weighted correlation network analysis, *BMC Bioinf.* 9 (2008) 559.
- [54] D. Szklarczyk, et al., The STRING database in 2011: functional interaction networks of proteins, globally integrated and scored, *Nucleic Acids Res.* 39 (Database issue) (2011) D561–D568.
- [55] Z. Wang, et al., Amino acid transporter SLC38A5 regulates developmental and pathological retinal angiogenesis, *Elife* (2022) 11.
- [56] T. Sniegowski, et al., SLC6A14 and SLC38A5 drive the glutaminolysis and serine-glycine-one-carbon pathways in cancer, *Pharmaceuticals* 14 (3) (2021).
- [57] G. Taurino, et al., The SLC38A5/SNAT5 amino acid transporter: from pathophysiology to pro-cancer roles in the tumor microenvironment, *Am. J. Physiol. Cell Physiol.* 325 (2) (2023) C550–c562.
- [58] Y.V. Bobryshev, et al., VCAM-1 expression and network of VCAM-1 positive vascular dendritic cells in advanced atherosclerotic lesions of carotid arteries and aortas, *Acta Histochem.* 98 (2) (1996) 185–194.
- [59] F. Clarke, et al., Protein tyrosine phosphatase PTPN22 is dispensable for dendritic cell antigen processing and promotion of T-cell activation by dendritic cells, *PLoS One* 12 (10) (2017) e0186625.
- [60] J.H. Wang, C. Kwas, L. Wu, Intercellular adhesion molecule 1 (ICAM-1), but not ICAM-2 and -3, is important for dendritic cell-mediated human immunodeficiency virus type 1 transmission, *J. Virol.* 83 (9) (2009) 4195–4204.
- [61] A.J. Moore, et al., A key role for IL-7R in the generation of microenvironments required for thymic dendritic cells, *Immunol. Cell Biol.* 95 (10) (2017) 933–942.
- [62] T.D. Holmes, et al., Licensed human natural killer cells aid dendritic cell maturation via TNFSF14/LIGHT, *Proc. Natl. Acad. Sci. U.S.A.* 111 (52) (2014) E5688–E5696.
- [63] W. Wei, et al., Gpr174 knockout alleviates DSS-induced colitis via regulating the immune function of dendritic cells, *Front. Immunol.* 13 (2022) 841254.
- [64] O. Cédile, et al., The chemokine receptor CCR2 maintains plasmacytoid dendritic cell homeostasis, *Immunol. Lett.* 192 (2017) 72–78.
- [65] M. Wu, H. Fang, S.T. Hwang, Cutting edge: CCR4 mediates antigen-primed T cell binding to activated dendritic cells, *J. Immunol.* 167 (9) (2001) 4791–4795.
- [66] A. Kowalczyk, C.A. D'Souza, L. Zhang, Cell-extrinsic CTLA4-mediated regulation of dendritic cell maturation depends on STAT3, *Eur. J. Immunol.* 44 (4) (2014) 1143–1155.
- [67] S. Dallari, et al., Src family kinases Fyn and Lyn are constitutively activated and mediate plasmacytoid dendritic cell responses, *Nat. Commun.* 8 (2017) 14830.
- [68] D.L. Krebs, et al., Lyn-dependent signaling regulates the innate immune response by controlling dendritic cell activation of NK cells, *J. Immunol.* 188 (10) (2012) 5094–5105.

- [69] C.L. Chu, C.A. Lowell, The Lyn tyrosine kinase differentially regulates dendritic cell generation and maturation, *J. Immunol.* 175 (5) (2005) 2880–2889.
- [70] E. Takacs, et al., Immunogenic dendritic cell generation from pluripotent stem cells by ectopic expression of Runx3, *J. Immunol.* 198 (1) (2017) 239–248.
- [71] S. Varghese, et al., The glutaminase inhibitor CB-839 (telaglenastat) enhances the antimelanoma activity of T-cell-mediated immunotherapies, *Mol. Cancer Therapeut.* 20 (3) (2021) 500–511.
- [72] N.A. Zumwalde, et al., Analysis of immune cells from human mammary ductal epithelial organoids reveals V δ 2+ T cells that efficiently target breast carcinoma cells in the presence of bisphosphonate, *Cancer Prev. Res.* 9 (4) (2016) 305–316.
- [73] A.C. Degnim, et al., Immune cell quantitation in normal breast tissue lobules with and without lobulitis, *Breast Cancer Res. Treat.* 144 (3) (2014) 539–549.
- [74] K.L. Lee, et al., Effects of cancer stem cells in triple-negative breast cancer and brain metastasis: challenges and solutions, *Cancers* 12 (8) (2020).
- [75] K.L. Lee, et al., Triple-negative breast cancer: current understanding and future therapeutic breakthrough targeting cancer stemness, *Cancers* 11 (9) (2019).
- [76] J.M. Brown, M.D. Wasson, P. Marcato, The missing Lnc: the potential of targeting triple-negative breast cancer and cancer stem cells by inhibiting long non-coding RNAs, *Cells* 9 (3) (2020).